nature neuroscience

RESOURCE



# Single-neuron labeling with inducible Cre-mediated knockout in transgenic mice

Paul Young[1,2], Li Qiu[1], Dongqing Wang[1], Shengli Zhao[1], James Gross[1,3] & Guoping Feng[1,4]

**To facilitate a functional analysis of neuronal connectivity in a mammalian nervous system that is tightly packed with billions of cells, we developed a new technique that uses inducible genetic manipulations in fluorescently labeled single neurons in mice. Our technique, single-neuron labeling with inducible Cre-mediated knockout (SLICK), is achieved by coexpressing a drug-inducible form of Cre recombinase and a fluorescent protein in a small subsets of neurons, thus combining the powerful Cre recombinase system for conditional genetic manipulation with fluorescent labeling of single neurons for imaging. Here, we demonstrate efficient inducible genetic manipulation in several types of neurons using SLICK. Furthermore, we applied SLICK to eliminate synaptic transmission in a small subset of neuromuscular junctions. Our results provide evidence for the long-term stability of inactive neuromuscular synapses in adult animals and demonstrate a Cre-loxP compatible system for dissecting gene functions in single identifiable neurons.**

The mammalian nervous system contains a heterogeneous mixture of billions of neurons that are interconnected by trillions of synapses. Techniques for revealing the morphological and electrophysiological properties of single neurons have overcome this complexity and helped to lay the foundations of modern neuroscience. Today, the sequencing of several mammalian genomes presents neuroscientists with unprecedented opportunities to determine the molecular mechanisms underlying the complex structure and function of the nervous system. Genetic manipulation in mice is a powerful tool for dissecting the roles of individual genes in the nervous system, and large scale projects with the ultimate goal of generating conditional-knockout alleles of all mouse genes are currently underway[1]. The difficulty, however, lies in the detailed analysis of the structure and function of mutant neurons in a brain that is tightly packed with billions of interconnected cells. Thus, the development of tools for conditional genetic manipulation of individual neurons in mice would greatly facilitate functional genomics in the nervous system. Furthermore, a wealth of genetically encoded tools is now available to both monitor and manipulate various properties of neurons[2–8]. Genetic approaches that allow the application of these tools in single identifiable neurons would greatly expand their utility in probing neuronal structure and function[9].

A major difficulty in carrying out genetic analyses on single neurons *in vivo* is the identification of the small numbers of genetically modified neurons among the masses of wild-type cells[10]. We previously generated transgenic mice in which small subsets of neurons are brightly labeled with fluorescent proteins by taking advantage of a transgenic phenomenon called 'position-effect variegation'[11]. The fluorescent labeling of isolated single neurons in a Golgi-like fashion in living animals permits the direct *in vivo* visualization and imaging of neuronal dynamics in accessible regions of the nervous system[12–15]. Here we describe a method that combines the fluorescent labeling of single neurons with inducible genetic manipulation in these same labeled neurons. This is done by using two copies of the *Thy1* promoter to simultaneously express CreER$^{T2}$, a drug-inducible form of the Cre recombinase enzyme[16], and yellow fluorescent protein (YFP) in the same cells. This method (SLICK) combines the powerful Cre/loxP system for carrying out conditional gene knockout or transgene expression with the labeling of single neurons with a fluorescent reporter to reveal their morphology. Genetic manipulation is spatially restricted to small subsets of labeled neurons and can be controlled temporally through administration of the activating drug, tamoxifen. We validated this method by showing efficient, tamoxifen-induced, Cre-mediated recombination in fluorescently labeled single neurons of SLICK mice. As a proof of principle for this approach, we used SLICK mice to manipulate neural activity *in vivo* by deleting the *choline acetyltransferase* (*Chat*) gene in subsets of labeled motor neurons. This approach reveals notable long-term stability of the neuromuscular synapse in the absence of synaptic transmission. Further, our study demonstrates a powerful genetic tool that is compatible with all Cre/loxP-based genetically modified mice.

## RESULTS

### Transgenic coexpression of Cre recombinase and YFP

The Cre/loxP site-specific recombinase system has been widely used to carry out both conditional gene knockout and conditional gene expression in mice[17]. Our goal was to develop transgenic mice in which it is possible to perform inducible genetic manipulation using the Cre/loxP system in small subsets of fluorescently labeled neurons

[1]Department of Neurobiology, Duke University Medical Center, Research Drive, Durham, North Carolina 27710, USA. [2]Department of Biochemistry, Biosciences Institute, University College Cork, Cork, Ireland. [3]Duke Neurotransgenic Laboratory and [4]Department of Pathology, Duke University Medical Center, Research Drive, Durham, North Carolina 27710, USA. Correspondence should be addressed to G.F. (feng@neuro.duke.edu) or P.Y. (p.young@ucc.ie).

Received 11 February; accepted 2 April; published online 4 May 2008; doi:10.1038/nn.2118

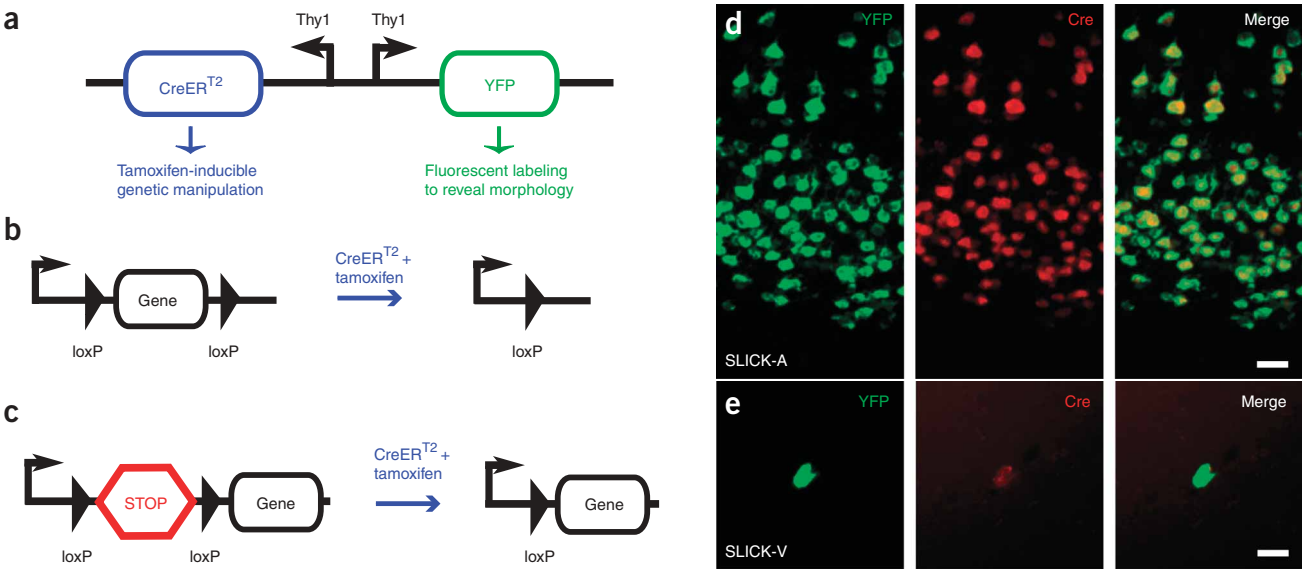


**Figure 1** Strategy used for coexpression of YFP and Cre in SLICK transgenic mice. (**a**) Schematic representation of the DNA construct that we used to generate SLICK transgenic mice. Two copies of the Thy1 promoter drive expression of YFP and the inducible form of Cre recombinase, CreER$^{T2}$. CreER$^{T2}$ consists of Cre recombinase fused to a modified ligand-binding domain from the estrogen receptor that can be activated by the synthetic ligand tamoxifen, but not by endogenous estrogens[16]. Tamoxifen administration can thus be used to control the timing of recombination. (**b**,**c**) Strategies to achieve conditional gene knockout and expression using the SLICK system. SLICK mice are first crossed to mice in which the expression of a gene of interest is controlled by Cre-mediated recombination. For gene knockout, part or all of the coding sequence of a gene of interest is flanked by two short *loxP* sequences (floxed) and is excised on Cre activation by tamoxifen (**b**). For conditional transgene expression, a transcriptional stop sequence (STOP cassette) is placed immediately upstream of the coding sequence of the transgene. Deletion of the stop cassette by activated Cre initiates transgene expression (**c**). (**d**,**e**) Double-fluorescent *in situ* hybridization for YFP (green) and Cre recombinase (red) in the cortex of SLICK-A (**d**) and hippocampus of SLICK-V (**e**) transgenic mice, respectively. Scale bar, 20 μm.

throughout the nervous system. With this goal in mind, we evaluated strategies to achieve transgenic coexpression of a fluorescent protein and CreER$^{T2}$, a tamoxifen-inducible form of Cre recombinase[16,18]. We reasoned that this would reveal the morphology of single labeled neurons, while simultaneously permitting Cre-mediated gene knockout or gene expression in these same cells on tamoxifen administration (**Fig. 1a–c**).

Our initial attempts to coexpress a fluorescent protein and CreER$^{T2}$ using the neuron-specific *Thy1* promoter in conjunction with an internal ribosome entry site did not allow both proteins to be coexpressed at high levels (data not shown). Therefore, we switched to a strategy in which the expression of the cDNAs for each protein was driven by separate copies of the *Thy1* promoter that were linked together in opposite orientations (back to back). One copy drove expression of the yellow fluorescent protein (YFP), and the other drove expression of CreER$^{T2}$ (**Fig. 1a**). Transgenic mice were generated using this construct and are hereafter referred to as SLICK transgenic mice. As this strategy relied on separate copies of the *Thy1* promoter to drive transcription of both mRNAs, it was not clear whether both mRNAs would be expressed in the same cells, especially when transcription is influenced by position-effect variegation. To test this, we carried out double fluorescent *in situ* hybridization to examine the expression of YFP and CreER$^{T2}$ mRNAs in SLICK mice (**Fig. 1d**). The expression of both mRNAs in the same cells was highly correlated; 96.2% (± 0.6%) of the YFP-expressing cells also expressed Cre, whereas 99% (± 0.3%) of Cre-positive cells expressed YFP. This tight correlation was also

**Table 1 Summary of the YFP expression patterns in seven lines of SLICK transgenic mice**

| | | Retina | | | SMG | | | Hippocampus | | Cerebellum | | | Olf |
|---|---|---|---|---|---|---|---|---|---|---|---|---|---|
| SLICK line | Motor axons | RGC | INL | DRG | Pre | Post | Cortex | CA1 | DG | Mossy | Purk | Gran | Mitral |
| SLICK-3 | All | Few | Few | Many | None | Few | Many | Many | None | Many | None | None | Few* |
| SLICK-A | Few* | Few | None | Few | None | None | Many | Many | Many | Many | None | None | None |
| SLICK-H | All | All | Many | All | All | Many | Many | All | Many | Many | Many | Many | Many |
| SLICK-I | All | All | n/d | All | Many* | Few* | Many | Many | Many | Many | Many | None | Many |
| SLICK-P | All | Many | n/d | Many | Many* | None | Many | Many | Many | Many | Many | None | Many |
| SLICK-V | Few | Few* | None | Few | None | None | Few* | Few* | Many | Few | None | Few | None |
| SLICK-X | Few | Few | None | Few | n/d | n/d | Few* | Few* | Many | Few | None | Few | None |

The extent of labeling is classified into three broad categories according to the percentage of neurons in the indicated population that are labeled. Few denotes < 10% labeled, many denotes 10–90% labeled and all denotes >90% labeled. * indicates neuronal populations with especially noteworthy labeling. DG, dentate granule cells; DRG, dorsal root ganglion; Gran, cerebellar granule cells; INL, inner nuclear layer; Mitral, mitral cells; Mossy, cerebellar mossy fibers; Olf, olfactory bulb; Post, postsynaptic; Pre, presynaptic; Purk, cerebellar purkinje cells; RGC, retinal ganglion cell; SMG, submandibular ganglion; n/d, not determined.

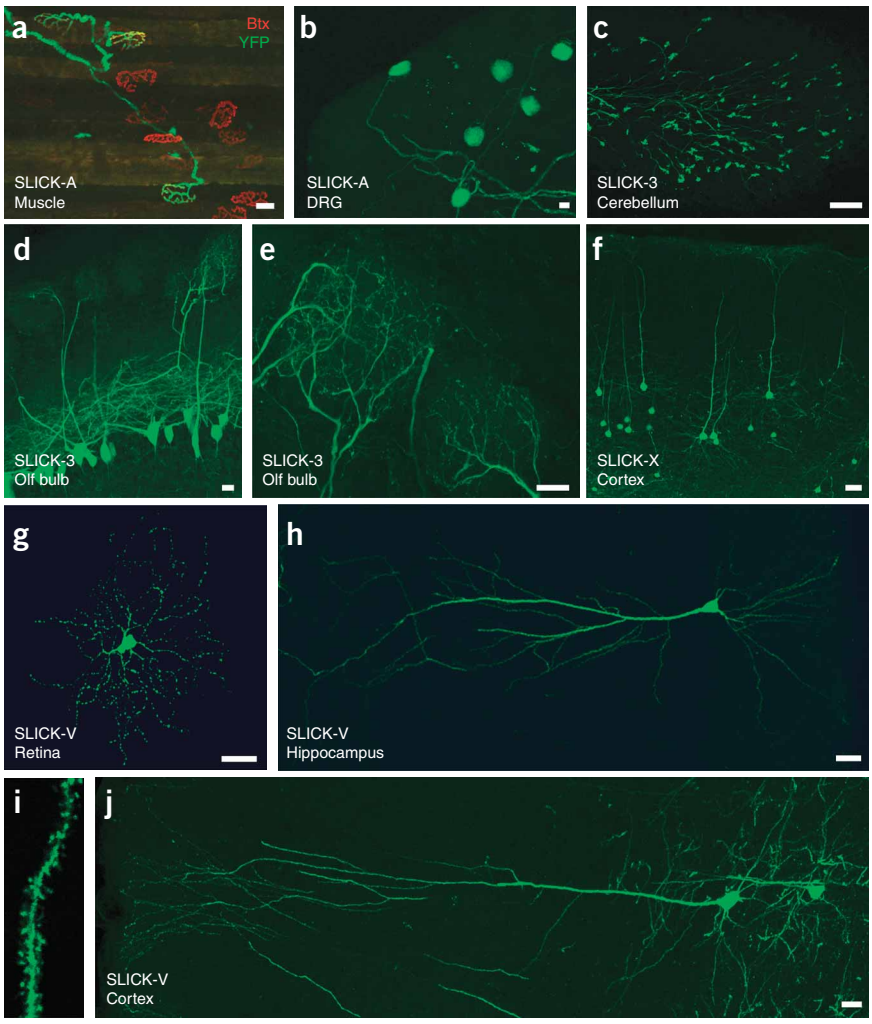


**Figure 2** YFP labeling of distinct neuronal populations in SLICK transgenic mice. (**a**) Labeling of motor axons in the latissimus dorsi muscle of the SLICK-A line (green). Co-staining for acetylcholine receptors with α-bungarotoxin at the neuromuscular junction (red) showed that only a subset of motor axons were labeled in this line. (**b**) YFP expression in a small number of dorsal root ganglion (DRG) neurons in the SLICK-A line. (**c**) Labeling of a subset of mossy fiber axons and nerve terminals in the granule cell layer of the cerebellum in the SLICK-3 line. (**d**,**e**) A small subset of YFP-expressing mitral cells in the olfactory bulb (Olf bulb) of SLICK-3 mice. A high-magnification view of the mitral cell apical dendrites in two glomeruli is shown (**e**). (**f**) Labeling of layer five cortical neurons in the SLICK-X line. (**g**) Bright YFP labeling of a small number of retinal ganglion cells in the retina of SLICK-V mice. (**h**–**j**) Extremely sparse labeling of pyramidal neurons in the hippocampus (**h**,**i**) and neocortex (**j**) of SLICK-V mice. Fine morphological features, such as dendritic spines, were readily discernable at higher magnification (**i**). Scale bars, 20 μm.

observed in lines in which expression was restricted to a very small subset of neurons (**Fig. 1e**).

## Fluorescent labeling of neurons in SLICK transgenic lines

We generated 30 lines of SLICK transgenic mice and examined fluorescent labeling of neurons throughout the nervous system of at least two mice from each line. YFP expression was confined primarily to projection neurons, with variations in the extent and brightness of labeling from line to line, as previously reported for the *Thy1* promoter[11]. Similar to other transgenic mice expressing various fluorescent proteins under the control of the Thy1 promoter (Thy1-XFP mice[11]), the expression patterns in SLICK mice were stably inherited in each line from generation to generation (**Supplementary Fig. 1** online). Although there is some variability in the number of labeled neurons between individuals in a line, the overall pattern of labeling does not change (**Supplementary Fig. 1**). We were primarily interested in the lines in which small subsets of neurons are brightly labeled so that genetic manipulation and imaging can be carried out in single neurons. Thus, most transgenic lines with weak or very widespread YFP expression were not maintained. However, one line (SLICK-H) with both widespread and strong expression of YFP has been maintained for possible use in experiments in which imaging of neurons is not required (the YFP-labeling patterns that we have observed in our different lines are summarized in **Table 1**).

To evaluate YFP expression in the peripheral nervous system of SLICK transgenic mice, we examined motor neurons, sensory neurons (dorsal root ganglion) and parasympathetic neurons (submandibular ganglion). Several lines were obtained in which restricted subsets of cells in these neuronal populations were labeled (**Fig. 2** and **Table 1**). In the SLICK-A line, a small subset of motor axons (<5%) were labeled in most muscles examined (**Fig. 2a**). Exceptions to this were the extraocular muscles of the eye, in which approximately 50% of axons express YFP. Similarly, a small number of dorsal root ganglion neurons were labeled in SLICK-A mice (**Fig. 2b**).

In the CNS, labeling of various subsets of neurons can similarly be observed in several lines. A subset of mitral cells (generally 1–3 mitral cells per glomerulus) in the olfactory bulb were labeled in the SLICK-3 line (**Fig. 2d**,**e**). In many of the glomeruli in this line, the fine structure of dendritic tufts originating from a single-labeled mitral cell could be visualized, making *in vivo* imaging of mitral cells by two-photon microscopy feasible (data not shown). This line also showed labeling in mossy fiber axons projecting to the granule cell layer of the cerebellum (**Fig. 2c**). The SLICK-V line showed much sparser labeling of neurons in the brain. For example, only 6–12 brightly labeled retinal ganglion cells were typically observed per retina (**Fig. 2g**). Brightly labeled single neurons were found more frequently in the hippocampus, and there was very sparse labeling of pyramidal neurons in several areas of the neocortex. (**Fig. 2h**,**j**). Labeled cells were also seen in many other regions of the brain, including the amygdala, brain stem and the inferior and superior colliculi (**Supplementary Fig. 2** online). The complete dendritic trees of pyramidal cells in the cortex and in the CA1 region of the hippocampus could be imaged in SLICK-V mice, and fine features such as dendritic spines were easily visualized (**Fig. 2i**). The SLICK-X line had a YFP-labeling pattern that was quite similar to SLICK-V in many parts of the brain, but with a higher number of labeled neurons in these areas compared with SLICK-V

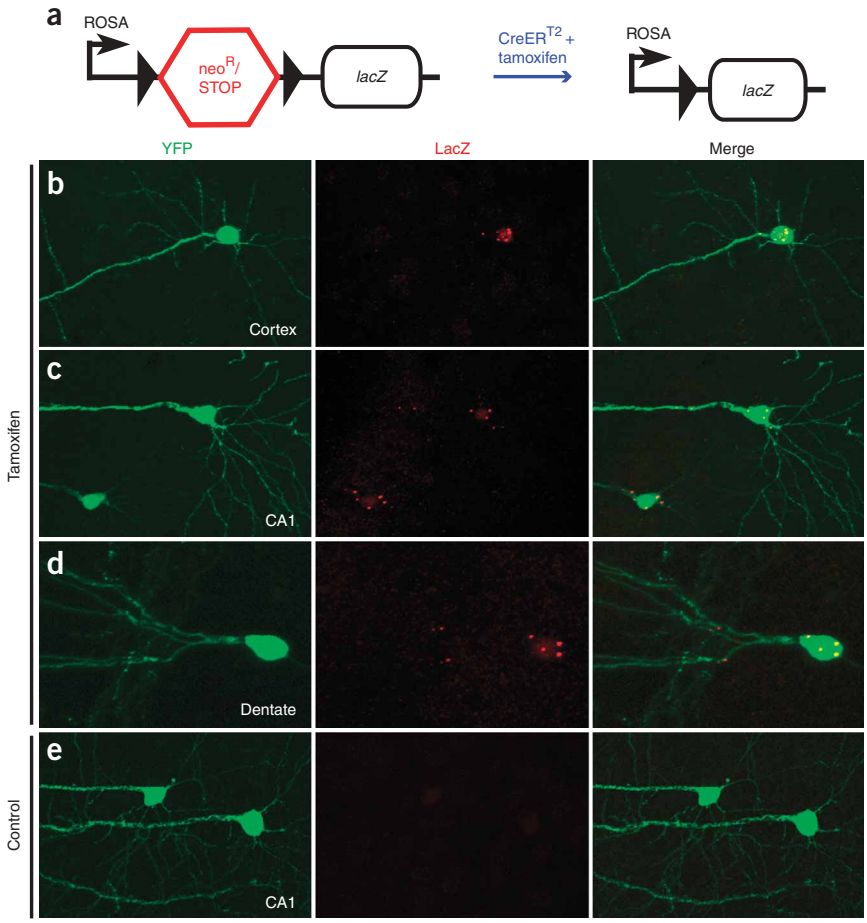


**Figure 3** Genetic manipulation in SLICK transgenic mice. (**a**) Schematic representation of the R26R Cre reporter strain[19]. A neomycin-resistance gene and transcriptional stop sequence are removed on Cre-mediated recombination to allow expression of the *lacZ* reporter gene coding for β-galactosidase. The black triangles represent *loxP* sites. SLICK-V transgenic mice that had been crossed to the R26R reporter were treated with either tamoxifen to induce Cre recombinase activity or corn oil as a control. (**b**–**e**) Efficient genetic manipulation as indicated by *lacZ* expression was seen in fluorescently labeled neurons of tamoxifen-treated mice (**b**–**d**), but not in control animals (**e**). A layer five cortical neuron (**b**), pyramidal neurons in the CA1 region of the hippocampus (**c**,**e**) and a granule cell in the dentate gyrus (**d**) are shown. 630× magnification for **b**–**e**.

(**Supplementary Fig. 3** online). In particular, a higher degree of labeling in the cortex of SLICK-X may be advantageous for transcranial *in vivo* imaging (**Fig. 2f**). In summary, the fluorescent labeling in SLICK transgenic mice reveals the detailed morphology of neurons in many regions of the nervous system, including several areas that are amenable to live *in vivo* imaging approaches (whole brain images showing YFP fluorescence in sagittal sections from SLICK-V and SLICK-X lines are shown in **Supplementary Figs. 2** and **3**).

### Validation of CreER$^{T2}$ function in SLICK mice

We next wanted to test whether it was possible to carry out inducible genetic manipulations in the fluorescently labeled neurons of SLICK transgenic mice. To do this we used the R26R Cre reporter strain[19]. In this strain, a *neomycin* gene flanked by loxP sites was placed upstream of a *lacZ* sequence coding for β-galactosidase and targeted to the *ROSA26* locus (**Fig. 3a**). Excision of the *neomycin* gene by Cre recombinase activity allows *lacZ* expression from the *ROSA26* promoter. Because this strain was generated using a 'knock-in' gene-targeting approach, there is only one copy of the reporter gene construct, unlike transgenic reporter lines in which multiple copies of the transgene are present. This allowed us to accurately determine recombination efficiency at a single locus, which is equivalent to Cre-mediated recombination for conditional gene knockout.

SLICK-V mice were crossed to the R26R reporter and double heterozygous animals were treated with tamoxifen to induce Cre activity (**Fig. 3a**). We administered tamoxifen or vehicle alone (corn oil) by oral gavage once a day, for 5 d consecutively. Recombination as indicated by *lacZ* expression was assayed by immunofluorescent staining for β-galactosidase 2 weeks after the final treatment with tamoxifen (**Fig. 3b**–**e**). *lacZ*-positive cells were never seen in vehicle-treated animals (**Fig. 3e**). In tamoxifen-treated animals, we observed robust *lacZ* expression in YFP-positive neurons (**Fig. 3b**–**d**) and only rarely observed *lacZ*-positive cells in which YFP fluorescence was not detected (<1% of all *lacZ*-positive cells; data not shown). Thus, the SLICK-V/R26R animals showed no 'leaky' reporter-gene expression, and Cre activity was inducible and confined to fluorescently labeled neurons as expected. Recombination occurred in 24–48 h after tamoxifen administration, whereas robust *lacZ* expression was observed by 5 d post-treatment (**Supplementary Fig. 4** online). We next quantified the efficiency of recombination in brightly fluorescent neurons from several brain regions of SLICK-V/R26R mice (**Table 2** and **Supplementary Fig. 5** online). The efficiency of recombination exceeded 95% in most of the neuronal populations examined (**Table 2**). Similar results were obtained for the SLICK-X line (**Table 2** and **Supplementary Fig. 6** online). The SLICK system therefore allows one to reliably identify and image genetically manipulated single neurons.

**Table 2 Efficiency of recombination assessed in SLICK-V and SLICK-X/R26R double-transgenic mice**

| | Brainstem | Thalamus | Hippocampus CA1 | Dentate gyrus | Cortex |
|---|---|---|---|---|---|
| SLICK-V | 98% (62/63) | 90% (17/19) | 96% (204/213) | 95% (131/138) | 95% (72/76) |
| SLICK-X | 97% (140/144) | 90% (150/166) | 93% (289/312) | 98% (643/659) | 92% (274/298) |

All brightly labeled YFP-positive cells in at least seven 50-μm sagittal sections were counted. The numbers in parentheses indicate the number of *lacZ*-positive cells / YFP-positive cells. Percentages were calculated from these numbers.

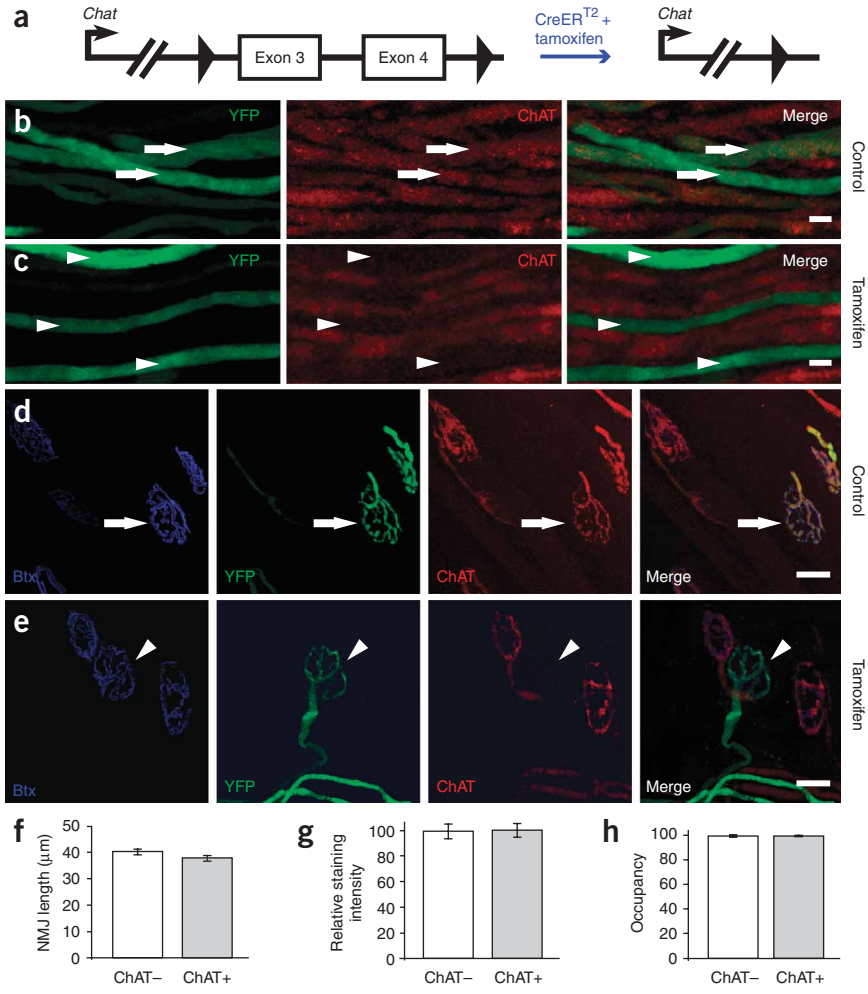


**Figure 4** Inhibition of neurotransmission in subsets of motor neurons through *Chat* knockout in SLICK-A mice. (**a**) Schematic representation of the conditional *Chat* allele. Exons 3 and 4 are deleted on Cre-mediated recombination. (**b**,**c**) Immunofluorescence staining for ChAT in segments of nerve entering the extraocular muscles. Efficient *Chat* knockout was observed in YFP-labeled motor axons of tamoxifen-treated (**c**), but not of control, animals (**b**). Arrows and arrowheads show ChAT-positive (ChAT+) and ChAT-negative (ChAT–) axons, respectively. (**d**,**e**) Staining of NMJs for ChAT and α-bungarotoxin (Btx; to label acetylcholine receptors). All nerve terminals showed strong ChAT staining in control animals, but *Chat* was specifically deleted from YFP-labeled terminals in tamoxifen-treated animals. The arrow and arrowhead show ChAT+ and ChAT– NMJs, respectively (**f**–**h**). Quantification of aspects of NMJ morphology for ChAT+ and ChAT– NMJs. The length of NMJs was determined as a measure of overall junction size in **f** ($n = 75$ junctions). Staining intensity for α-bungarotoxin was quantified as a measure of junctional acetylcholine receptor density in **g** ($n = 40$ junctions). We measured the area of α-bungarotoxin staining at NMJs that were occupied by YFP-labeled ChAT+ and ChAT– presynaptic nerve terminals ($n = 97$ junctions, **h**). Data from at least three muscles were used in all quantifications. Scale bars, 20 μm. Error bars in **f**, **g** and **h** represent the s.e.m.



## Conditional gene knockout in SLICK mice

Understanding the mechanisms by which neural activity influences the formation and plasticity of neural circuits is a major focus of neuroscience research[20,21]. To address this issue using the SLICK system, we took advantage of mice carrying a conditional-knockout allele of the *Chat* gene[22] (**Fig. 4a**). *Chat* is required for the synthesis of the neurotransmitter acetylcholine, and genetic ablation of *Chat* has been shown to eliminate neurotransmission at cholinergic synapses such as the neuromuscular junction (NMJ), resulting in neonatal lethality[22,23]. To examine the consequences of long-term inhibition of neurotransmission at adult neuromuscular synapses, we used the SLICK-A line to knock out *Chat* in a small subset of YFP-labeled motor neurons. SLICK-A *Chat*$^{loxP/-}$ mice were treated with either tamoxifen to induce *Chat* knockout or with corn oil as a control (**Fig. 4b–e**). Motor axons and neuromuscular synapses were examined 8 weeks after tamoxifen treatment. ChAT expression was monitored by immunofluorescent staining and postsynaptic acetylcholine receptors were labeled with α-bungarotoxin. In untreated control animals, ChAT was present in both YFP-labeled (arrows) and unlabeled axons and in nerve terminals (**Fig. 4b**,**d**). In contrast, ChAT was undetectable in 99% (111/112) of YFP-labeled motor axons and 97% (73/75) of YFP-labeled nerve terminals in tamoxifen-treated animals (arrowheads; **Fig. 4c**,**e**). ChAT was present in almost all YFP-negative axons and terminals of tamoxifen-treated animals (**Fig. 4b**,**d**), although ChAT was occasionally not detectable in non–YFP-labeled axons and terminals (data not shown, see **Supplementary Discussion** online). Similar overall results for *Chat* knockout were observed 4 weeks after tamoxifen administration (data not shown). Thus, NMJs examined at an 8-week time point would have been completely depleted of ChAT for at least 4 weeks. In summary, extremely efficient recombination of the floxed *Chat* allele in YFP-expressing cells was observed. This demonstrates that the SLICK system can be used to achieve gene knockout at rates that are as high, or even higher than, those observed for reporter gene expression (see **Table 2**).

To determine whether NMJ stability is altered by long-term inhibition of neurotransmission in a subset of motorneurons, we compared YFP-labeled ChAT-negative NMJs to unlabeled ChAT-positive NMJs. As a measure of overall NMJ size, we quantified the maximal length of NMJs as revealed by α-bungarotoxin labeling. We also examined the expression levels of postsynaptic acteylcholine receptors by quantifying the intensity of α-bungarotoxin staining. We found no significant difference between ChAT-positive and ChAT-negative junctions for either of these parameters ($P > 0.05$; **Fig. 4f**,**g**). We next examined the morphology of YFP-expressing ChAT-negative nerve terminals. We found that the YFP labeling of nerve terminals precisely matched the postsynaptic α-bungarotoxin staining at ChAT-negative junctions. The occupancy of α-bungarotoxin–labeled postsynaptic sites by ChAT-negative nerve terminals was 99.7% ($n = 97$ junctions). This was identical to the occupancy of postsynaptic sites by YFP-labeled ChAT-positive terminals in untreated control animals (**Fig. 4h**). Thus, there is no evidence of retraction of inactive terminals from NMJs. Moreover, we did not observe any aberrant growth or sprouting of inactive axons or any gross abnormalities in the complexity or structure of inactive terminals. In summary, 8 weeks following *Chat* knockout, inactive

*Chat*$^{-/-}$ NMJs were morphologically indistinguishable from neighboring active junctions and there was no evidence of replacement of inactive terminals by active ones.

## DISCUSSION

Genetic manipulation in mice has proven to be a powerful tool for dissecting mechanisms that underlie the development, maintenance and plasticity of neuronal connectivity[24]. Here we describe the generation of SLICK transgenic mice that allow genetically manipulations in single neurons that are brightly labeled with YFP. Recombination efficiencies of greater than 95% were observed for both inducible transgene expression and gene knockout. The ability to genetically manipulate labeled neurons in such a precise manner has several advantages. First, the Golgi-like labeling with YFP permits the analysis of detailed morphology and synaptic connections of individual mutant neurons. Second, the restriction of genetic manipulation to a labeled, small subset of neurons allows analysis to be carried out in a predominantly wild-type background, preventing large-scale disruption of neural circuits and allowing cell-autonomous gene function to be distinguished from indirect effects of widespread gene knockout. This should facilitate the examination of competition between mutant and wild-type neurons in developmental processes such as synapse formation and elimination. Third, the inducible nature of genetic manipulations using the SLICK system permits gene function to be analyzed at late developmental or adult stages, thereby avoiding the potential complications of embryonic lethality, early developmental defects or secondary compensatory mechanisms. Another important feature of the SLICK system is that the YFP labeling of neurons is constitutive. This allows labeled neurons from untreated animals to be used as controls for genetically manipulated cells. Furthermore, *in vivo* imaging of YFP-labeled neurons should make it possible to image the same cells before and after a genetic manipulation, allowing the neuronal properties to be examined in the presence and absence of a given gene in the same neuron *in vivo*. Such time-lapse imaging of genetically manipulated neurons will also allow dynamic aspects of cellular morphology and synaptic plasticity to be studied.

The goal of our method is similar to that of a recently described technique termed mosaic analysis with double marker (MADM)[10]. Mosaic analysis makes use of mitotic recombination to generate clones of cells that are homozygous null for a gene of interest and has been widely used in *Drosophila*[25]. MADM is an adaptation of mosaic analysis for use in mice. The goal of both MADM and SLICK is to carry out genetic manipulations in fluorescently labeled populations of cells. However, there are many intrinsic differences between the two methods. For example, MADM operates in mitotic cells and is mostly applicable in neurons at early developmental stages, when neuronal precursors are still dividing. SLICK, in comparison, would be more applicable in late embryonic, postnatal and adult mice, as it relies on the *Thy1* promoter, which is most active at these stages. For gene-knockout experiments, the sets of genes that can be used by each technique are different. MADM can be used for all types of mutations (targeted, spontaneous or chemically induced) once markers are eventually placed on each arm of all mouse chromosomes. In comparison, SLICK is compatible with all floxed conditional-knockout alleles, but not with other types of mutations. MADM has the advantage that it is not restricted to neurons and can, in principle, be used in any cell or tissue. SLICK is neuron specific, but has the advantage of being able to temporally control genetic manipulations in defined types of neurons. Thus, although the goals of both methods are broadly similar, in practice they are likely to find different, but very complementary, applications in neuroscience research.

To demonstrate the utility of SLICK for gene knockout, we used the system to inhibit cholinergic neurotransmission by knocking out essential exons in the *Chat* gene[22]. This prevented acetylcholine synthesis, effectively silencing cholinergic neurons. Global disruption of cholinergic transmission is lethal because it results in respiratory failure[22,23]. We avoided lethality by using the SLICK-A line of mice to restrict *Chat* knockout to a very small subset of YFP-labeled motor neurons in most muscles. This provided us with a unique opportunity to inhibit neurotransmission *in vivo* for long periods of time in subsets of nerve terminals, while leaving the activity of their neighbors unperturbed. We examined the consequences of this manipulation on the stability of the NMJ. We found that the gross morphology of the NMJ was unchanged under such conditions. There were no alterations in the level of receptor expression at silenced junctions, consistent with observations following short-term pharmacological inhibition of action potentials[26,27]. We also considered the possibility that active axons might invade or take over inactive NMJs, similar to the manner in which denervated NMJs can be innervated by sprouting axons from intact neighboring junctions[28]. However, we found no evidence of *Chat*$^{-/-}$ nerve terminals vacating inactive junctions, and we did not find active axons replacing inactive ones (see **Supplementary Discussion**). In conclusion, the adult NMJ remains extremely stable for long periods in the absence of neurotransmission, despite potential competition from neighboring active nerve terminals.

In addition to its use for targeted gene knockout, SLICK can be used to target expression of any gene of interest to single, fluorescently labeled neurons *in vivo*. Many genetically encoded tools to both monitor and manipulate various physiological properties of neurons have been developed in recent years[2–8,29–32]. These include fluorescent reporters of synaptic transmission and ion concentrations, as well as reagents for modulating neuronal excitability and neurotransmitter release. SLICK will allow expression of such probes in single neurons *in vivo*, while simultaneously revealing the morphology of the neurons for imaging or identifying them for electrophysiological analysis. Used in this manner, SLICK will permit many genetically encoded probes to be applied with single-cell resolution in mice for the first time. Although some fluorescent reporters are based on YFP and would not be compatible with the SLICK mice described here, this problem could be circumvented by generating SLICK mice that express spectrally distinct fluorescent proteins[33]. SLICK therefore has the potential to increase the scope and utility of a wide variety of recently developed tools for monitoring and manipulating neurons and neural circuits.

SLICK is based on the popular Cre/loxP system that has been used extensively to achieve conditional gene knockout in mice[17,34,35]. The availability of mice harboring conditional-knockout alleles is continually increasing and a large-scale project to generate 'floxed' conditional-knockout alleles is underway[1]. The SLICK system can be used to tap into this resource and should permit cellular phenotypes to be studied in these mice at the single-neuron level. Thus, SLICK has considerable potential as a functional genomics tool for studying function and dysfunction of the nervous system.

## METHODS

**Generation of transgenic DNA constructs.** The Thy1 vector has been described previously and was provided to us by P. Caroni (Friedrich Miescher Institute for Biomedical Research)[11,36]. The vector pCreER$^{T2}$, containing the CreER$^{T2}$ coding sequence, was obtained from D. Metzger and P. Chambon (Institut de Génétique et de Biologie Moléculaire et Cellulaire)[16]. To generate the Thy1-YFP;Thy1-CreER$^{T2}$ double promoter construct, CreER$^{T2}$ was cut

from pCre-ER$^{T2}$ using *Eco*RI and cloned into the *Xho*I site of the Thy1 vector by blunt-end ligation. Thy1-YFP was generated as previously described[11]. Thy1-CreER$^{T2}$ and Thy1-YFP were then joined via an *Eco*RI site at the 5′ end of the Thy1 promoter. The final construct was linearized using *Not*I to remove the vector backbone before injection into oocytes.

**Mice.** SLICK transgenic mice were generated by injection of gel-purified DNA into fertilized oocytes using standard techniques[37]. Embryos for injection were obtained by mating (C57BL6/J and CBA) F1 hybrids. Transgenic founders were backcrossed to C57BL6/J mice for analysis of expression patterns. The primers and protocols used for genotyping are described in the **Supplementary Methods** online. The R26R line of Cre reporter mice[19] was from Jackson Laboratory (stock no. 003474). *Chat* conditional-knockout mice were obtained from J. Sanes (Harvard University)[22]. Experiments involving animals were conducted in accordance with the institutional protocols of Duke University. Animal experiments at University College Cork were approved by the University Ethics Committee and conducted under a license from the Department of Health and Children.

***In situ* hybridization.** Probe sequences comprising the complete coding sequences of YFP and Cre recombinase were cloned into pBluescript SKII vector (Stratagene). Digoxygenin- or fluorescein-labeled RNA probes were generated by *in vitro* transcription using the MaxiScript kit (Ambion) according to the manufacturer's instructions. For *in situ* hybridization, fresh tissues were dissected and quickly embedded and frozen in OCT compound (Tissue-Tek). We cut 20-μm sections on a Leica CM 1850 cryostat, fixed them for 5 min with 4% paraformaldehyde (wt/vol) in phosphate-buffered saline (PBS), and rinsed the sections three times in PBS. Double-fluorescent *in situ* hybridization was carried out using the tyramide signal-amplification system (Perkin Elmer). YFP mRNA was detected using a fluorescein-labeled probe and fluorescein-tyramide. Cre mRNA was detected using a digoxygenin-labeled probe and Cy3-tyramide. Images were acquired on a Zeiss Axioskop 2 fluorescent microscope using a 20× objective.

**Fluorescence imaging of SLICK mice.** For imaging of YFP fluorescence, mice were anesthetized and perfused through the heart, first with lactated Ringer's solution, and then with 4% paraformaldehyde (wt/vol). Images of muscles, dorsal root ganglia and retinas were taken from whole-mount tissues. For brains, 100-μm sections were cut using a vibrotome. Confocal images of both whole-mount tissue and sections were acquired on a Nikon Eclipse confocal microscope using 20× and 63× objectives. For two-color imaging of NMJs, acetylcholine receptors were labeled with rhodamine-conjugated α-bungarotoxin (1:10,000) for 2–3 h and washed three times in PBS. We carried out three-color imaging of muscles stained for ChAT on a Leica DM IRE2 confocal microscope using a HCX PLAPO 63× objective. YFP was excited using the 488-nm laser line and fluorescence emission collected between 508 and 550 nm. Cy3 was excited at 543 nm and fluorescence was collected between 555 and 627 nm. Alexa647 was excited at 633 nm and fluorescence was collected between 650 and 750 nm.

**Antibodies and immunohistochemistry.** Details of antibodies and protocols for immunohistochemistry are described in the **Supplementary Methods**.

**Tamoxifen administration.** Tamoxifen (Sigma, catalog no. T5648) was dissolved in corn oil (Kroger brand) at a concentration of 20 mg ml$^{-1}$ by rocking overnight at room temperature (20–25 °C). This was stored at room temperature for immediate use. Adult mice were administered 0.25 mg per g of body weight of tamoxifen per day by oral gavage for 5 d. For induction of recombination in SLICK-V/R26R mice, a second 5-d treatment was carried out 2 weeks after the first. SLICK-V/R26R mice were 12–16 weeks old on the date of the first treatment. To induce *Chat* gene knockout, mice were treated with tamoxifen for one period of 5 d at 10 weeks of age. These mice were then killed for analysis 5 or 9 weeks later.

**Image analysis and quantification.** We analyzed our *in situ* hybridization data and β-galactosidase immunohistochemistry by manually counting cells in merged two-color images that were created using Adobe Photoshop software. The selection of the cells to be counted was performed in a blinded manner before the images were merged. For determining the recombination efficiency in SLICK-V/R26R mice, we considered only bright cells that would be suitable for imaging of detailed cellular morphology.

Analysis of *Chat* knockout efficiency and NMJ structure was carried out entirely on whole-mount stained extraocular muscles. This was because the higher degree of labeling in these muscles provides ChAT-positive and ChAT-negative NMJs in approximately equal numbers for statistical analysis. To examine NMJs, we collected *z* series of confocal images and made maximum intensity projections of each series. All image analysis was carried out using ImageJ software. The size of ChAT-positive and ChAT-negative NMJs from the same muscle were quantified by measuring the maximal dimension of the α-bungarotoxin staining. Statistical comparison of ChAT-positive and ChAT-negative junction size was performed using an unpaired Student's *t*-test. Quantification of acetylcholine receptor density was carried out by measuring the fluorescence intensity from pairs of ChAT-positive and ChAT-negative NMJs in the same image. The same threshold was applied to the entire image and the areas with NMJs were selected using the wand tool in ImageJ and the average pixel intensity over an entire NMJ was then measured. We used only NMJs laying flat on the muscle fiber and pairs of nearby ChAT-positive and ChAT-negative NMJs at a similar focal depth for analysis. Statistical analysis was carried out using a paired *t*-test. Occupancy of NMJs by nerve terminals was calculated by making a line tracing of the pretzel-like pattern of bungarotoxin staining, including all branches using ImageJ. The length of this trace was measured and compared with a line tracing of the nerve terminal on the basis of the YFP fluorescence.

**Online resources and availability of SLICK mice.** Data describing neuronal labeling and recombination patterns in various SLICK mouse lines is available on the Feng Laboratory website (http://guopingfenglab.net/resources.html). The SLICK-A (#007606) and SLICK-V (#007610) lines are currently available from Jackson Laboratory (http://jaxmice.jax.org/). For information about the availability of other lines and how to request them, please see the Feng Laboratory website.

*Note: Supplementary information is available on the Nature Neuroscience website.*

**ACKNOWLEDGMENTS**

We thank J. Sanes for providing the *Chat* conditional-knockout mice and the antibody to β-galactosidase. We thank A. Mizrahi for performing two-photon imaging of SLICK-3 mice and R. Kotloski for advice regarding tamoxifen administration. We also thank the Duke Neurotransgenic Core Facility for generating the SLICK mice. We thank J. McNamara, M.D. Ehlers and M. McCaffrey for access to confocal microscopes. We are grateful to B. Arenkiel, M.D. Ehlers, A. West, K. Dean and members of the Feng laboratory for critically reading and discussing the manuscript. This work was supported by the Ruth K. Broad Biomedical Research Foundation, the Science Foundation Ireland and the US National Institutes of Health.

**AUTHOR CONTRIBUTIONS**

P.Y. and G.F. conceived the SLICK method, designed the experiments and wrote the manuscript. P.Y. and J.G. generated the SLICK transgenic mice. P.Y., L.Q., S.Z. and D.W. characterized the SLICK mice. P.Y. and S.Z. carried out the quantification and data analysis.

Published online at http://www.nature.com/natureneuroscience
Reprints and permissions information is available online at http://npg.nature.com/reprintsandpermissions

1. International Mouse Knockout Consortium. Collins, F.S., Rossant, J. & Wurst, W. A mouse for all reasons. *Cell* **128**, 9–13 (2007).
2. Brecht, M. *et al.* Novel approaches to monitor and manipulate single neurons *in vivo*. *J. Neurosci.* **24**, 9223–9227 (2004).
3. Callaway, E.M. A molecular and genetic arsenal for systems neuroscience. *Trends Neurosci.* **28**, 196–201 (2005).
4. Deisseroth, K. *et al.* Next-generation optical technologies for illuminating genetically targeted brain circuits. *J. Neurosci.* **26**, 10380–10386 (2006).
5. Marek, K.W. & Davis, G.W. Controlling the active properties of excitable cells. *Curr. Opin. Neurobiol.* **13**, 607–611 (2003).
6. Miesenbock, G. Genetic methods for illuminating the function of neural circuits. *Curr. Opin. Neurobiol.* **14**, 395–402 (2004).
7. Miyawaki, A. Fluorescence imaging of physiological activity in complex systems using GFP-based probes. *Curr. Opin. Neurobiol.* **13**, 591–596 (2003).

8. Luo, L., Callaway, E.M. & Svoboda, K. Genetic dissection of neural circuits. *Neuron* **57**, 634–660 (2008).
9. Young, P. & Feng, G. Labeling neurons *in vivo* for morphological and functional studies. *Curr. Opin. Neurobiol.* **14**, 642–646 (2004).
10. Zong, H., Espinosa, J.S., Su, H.H., Muzumdar, M.D. & Luo, L. Mosaic analysis with double markers in mice. *Cell* **121**, 479–492 (2005).
11. Feng, G. *et al.* Imaging neuronal subsets in transgenic mice expressing multiple spectral variants of GFP. *Neuron* **28**, 41–51 (2000).
12. Grutzendler, J., Kasthuri, N. & Gan, W.B. Long-term dendritic spine stability in the adult cortex. *Nature* **420**, 812–816 (2002).
13. Kasthuri, N. & Lichtman, J.W. Structural dynamics of synapses in living animals. *Curr. Opin. Neurobiol.* **14**, 105–111 (2004).
14. Trachtenberg, J.T. *et al.* Long-term *in vivo* imaging of experience-dependent synaptic plasticity in adult cortex. *Nature* **420**, 788–794 (2002).
15. Mizrahi, A. & Katz, L.C. Dendritic stability in the adult olfactory bulb. *Nat. Neurosci.* **6**, 1201–1207 (2003).
16. Feil, R., Wagner, J., Metzger, D. & Chambon, P. Regulation of Cre recombinase activity by mutated estrogen receptor ligand-binding domains. *Biochem. Biophys. Res. Commun.* **237**, 752–757 (1997).
17. Branda, C.S. & Dymecki, S.M. Talking about a revolution: the impact of site-specific recombinases on genetic analyses in mice. *Dev. Cell* **6**, 7–28 (2004).
18. Metzger, D. & Chambon, P. Site- and time-specific gene targeting in the mouse. *Methods* **24**, 71–80 (2001).
19. Soriano, P. Generalized *lacZ* expression with the ROSA26 Cre reporter strain. *Nat. Genet.* **21**, 70–71 (1999).
20. Burrone, J. & Murthy, V.N. Synaptic gain control and homeostasis. *Curr. Opin. Neurobiol.* **13**, 560–567 (2003).
21. Hua, J.Y. & Smith, S.J. Neural activity and the dynamics of central nervous system development. *Nat. Neurosci.* **7**, 327–332 (2004).
22. Misgeld, T. *et al.* Roles of neurotransmitter in synapse formation: development of neuromuscular junctions lacking choline acetyltransferase. *Neuron* **36**, 635–648 (2002).
23. Brandon, E.P. *et al.* Aberrant patterning of neuromuscular synapses in choline acetyltransferase–deficient mice. *J. Neurosci.* **23**, 539–549 (2003).
24. Chen, C. & Tonegawa, S. Molecular genetic analysis of synaptic plasticity, activity-dependent neural development, learning, and memory in the mammalian brain. *Annu. Rev. Neurosci.* **20**, 157–184 (1997).
25. Lee, T. & Luo, L. Mosaic analysis with a repressible cell marker for studies of gene function in neuronal morphogenesis. *Neuron* **22**, 451–461 (1999).
26. Wang, X. *et al.* Prolongation of evoked and spontaneous synaptic currents at the neuromuscular junction after activity blockade is caused by the upregulation of fetal acetylcholine receptors. *J. Neurosci.* **26**, 8983–8987 (2006).
27. Wang, X. *et al.* Activity-dependent presynaptic regulation of quantal size at the mammalian neuromuscular junction *in vivo*. *J. Neurosci.* **25**, 343–351 (2005).
28. Son, Y.J. & Thompson, W.J. Nerve sprouting in muscle is induced and guided by processes extended by Schwann cells. *Neuron* **14**, 133–141 (1995).
29. Johns, D.C., Marx, R., Mains, R.E., O'Rourke, B. & Marban, E. Inducible genetic suppression of neuronal excitability. *J. Neurosci.* **19**, 1691–1697 (1999).
30. Sweeney, S.T., Broadie, K., Keane, J., Niemann, H. & O'Kane, C.J. Targeted expression of tetanus toxin light chain in *Drosophila* specifically eliminates synaptic transmission and causes behavioral defects. *Neuron* **14**, 341–351 (1995).
31. Arenkiel, B.R. *et al. In vivo* light-induced activation of neural circuitry in transgenic mice expressing channelrhodopsin-2. *Neuron* **54**, 205–218 (2007).
32. Wang, H. *et al.* High-speed mapping of synaptic connectivity using photostimulation in Channelrhodopsin-2 transgenic mice. *Proc. Natl. Acad. Sci. USA* **104**, 8143–8148 (2007).
33. Shaner, N.C. *et al.* Improved monomeric red, orange and yellow fluorescent proteins derived from *Discosoma* sp. red fluorescent protein. *Nat. Biotechnol.* **22**, 1567–1572 (2004).
34. Lewandoski, M. Conditional control of gene expression in the mouse. *Nat. Rev. Genet.* **2**, 743–755 (2001).
35. Sauer, B. Inducible gene targeting in mice using the Cre/lox system. *Methods* **14**, 381–392 (1998).
36. Caroni, P. Overexpression of growth-associated proteins in the neurons of adult transgenic mice. *J. Neurosci. Methods* **71**, 3–9 (1997).
37. Hogan, B., Constantini, F. & Lacey, E. Production of transgenic mice. in *Manipulating the Mouse Embryo: A Laboratory Manual* (eds Hogan, B., Constantini, F. & Lacey, E.) 217–252 (Cold Spring Harbor Laboratory Press, Cold Spring Harbor, New York, 1994).